EOSC 453 Assignment 2

Volcanic Eruptions and Climate Change

E. Giroud-Proeschel - 123456789
P. Matlashewski - 45701109
M. Ormerod - 16265167

November 19, 2020

Contents

1 Introduction **2**

2 Results **2**
2.1 Steady-State Climate Model: No Volcanism . . . 2
2.2 Climate Model Following Single Volcanic Eruption . . . 3
2.3 Snowball Earth: Stochastic Volcanism and Temperature-Dependent Albedo . . . 4

3 Discussion **6**
3.1 Steady-State Climate Model: No Volcanism . . . 6
3.2 Climate Model Following Single Volcanic Eruption . . . 7
3.3 Snowball Earth: Stochastic Volcanism and Temperature-Dependent Albedo . . . 7

4 Conclusion **7**
4.1 Future Work . . . 7

5 Ancillary Information **7**
5.1 Author Contributions . . . 7
5.2 Algorithm Development . . . 7
5.3 Data . . . 8
5.3.1 Model Equations . . . 8
5.3.2 Equilibrium Temperatures: Steady State Model . . . 8
5.3.3 Eruption Times Series . . . 9
5.3.4 Parameters . . . 10

6 References **11**

1 Introduction

Anthropogenic global warming is an identifier of climate change and has manifested as a defining issue of our time; intensifying the frequency and severity of extreme weather events, producing sea-level rise with the potential to displace millions, causing the loss of large freshwater reservoirs, reducing biodiversity in key biomes, among other effects. Though the question of why, and how, climate change operates, and what we can do to mitigate its effect on the Earth of our lifetime, is an arduously nonlinear problem that climate scientists have battled with for decades, both in the laboratory and in politics. One of the questions within this contention is how large local out-gassing events of volatile aerosols during volcanic eruptions, like carbon dioxide and sulfur dioxide, have historically affected the Earth, from the last ice-age to the explosive evolution following it. Here we have developed a simple radiative energy balance model for the Earth in order to investigate the effects of volcanism on this energy balance's behaviour. This model is inspired by the work of Russian climatologist Mikhail I. Budyko of the Lenningrad Geophysics Observatory, who discovered the ice-albedo feedback mechanism underlying climate change through his pioneering of studies on global climate using physical models of equilibrium (Budyko 1969).

In this report, we will investigate perturbations to our climate model via volcanic forcing. This will take three forms. We will begin with a presently undisturbed model that approaches steady-state. Then we analyze the effects of an added perturbation of volcanic aerosols derived from data collected from the 1982 El Chichón and Pinatubo eruptions published in Robock 2000. Finally, we will implement a parameterization of temperature-dependent albedo in conjunction with a Poisson distribution of volcanic eruptions, temporally and spatially, to simulate a snowball Earth scenario. WE SHOULD ADD A BIT ABOUT OUR GENERAL ASSUMPTIONS HERE

2 Results

In this section, we will report on data obtained via our three forms of volcanic perturbations and describe the behaviours of these perturbations within the context of the data itself.

2.1 Steady-State Climate Model: No Volcanism

By passing initial condition temperatures calculated through our model with suppressed inter-zonal transfer (See Table 2) to our steady-state model where inter-zonal transfer is allowed, we solve for the equilibrium temperatures by integrating forward in time (Figure 1).

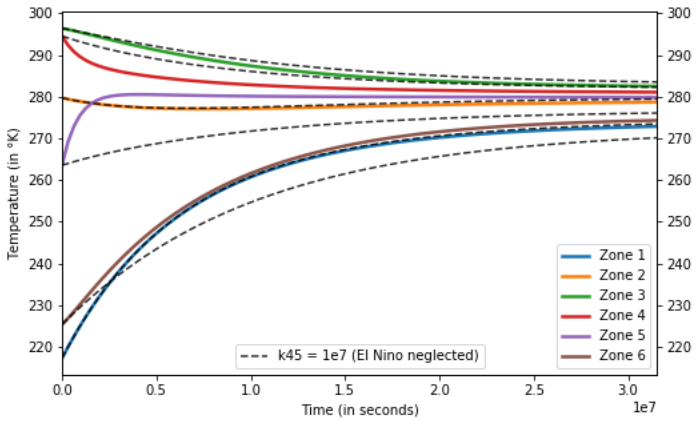

Figure 1: Equilibrium solution for 6-zoned Earth climate model. Zone 1 marks the southernmost band at $60 - 90°$S while zone 6 represents the northernmost band at $60 - 90°$N. Zones 2-5 are bands covering $30°$ intervals between zones 1 and 6 (See Figure 7).

There are a few key observations to note. The first is that a larger transfer coefficient (**??**), representing the northern Gulf Stream between zones 4 and 5, produces a large initial temperature gradient in these zones relative to the others (solid colour lines in Figure 1). The second is that the highest temperature zones at equilibrium are 3 and 4, and the lowest temperature zones at equilibrium are 6 and 1. All zones approach an equilibrium temperature between 274.1°K and 282.3°K after a model year. (Table 3). By reducing the inter-zonal transfer coefficient between zones 4 and 5 (dashed lines in Figure 1), we can alter the characteristics of a few zones dramatically. The most obvious of which are zones 4, 5, and, perhaps surprisingly, zone 6. These alterations include a reduction in the initial rate of change in temperature and will be analyzed further in Section 3.1.

2.2 Climate Model Following Single Volcanic Eruption

To introduce the effect of volcanism to our model, we add an occlusion factor, $\phi(t)$, to each zone that reduces total incoming solar radiation (Figure 2). $\phi_k(t)$ varies in initial magnitude and onset time based on proximity to the zone in which the eruption occurs. Alternatively, an eruption in zone 3 will have a reduced effect in zone 4 and 2 to simulate the thinning of aerosol density as the cloud spreads, and the aerosols have a travel time before the effect is felt in adjacent zones. $\phi(t)$ follows a $\frac{1}{t^2}$ fit to eruption data from Robock 2000 such that $\lim_{t\to\infty} \phi(t) = 1$. Figure 3 shows our solution post eruption.

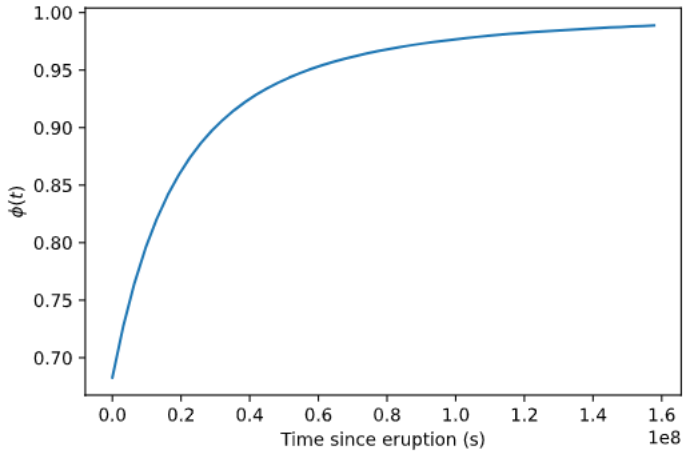

Figure 2: Plot of $\phi(t)$; occlusion factor. An occlusion factor of 0.7 represents a 30% reduction in total incoming solar radiation.

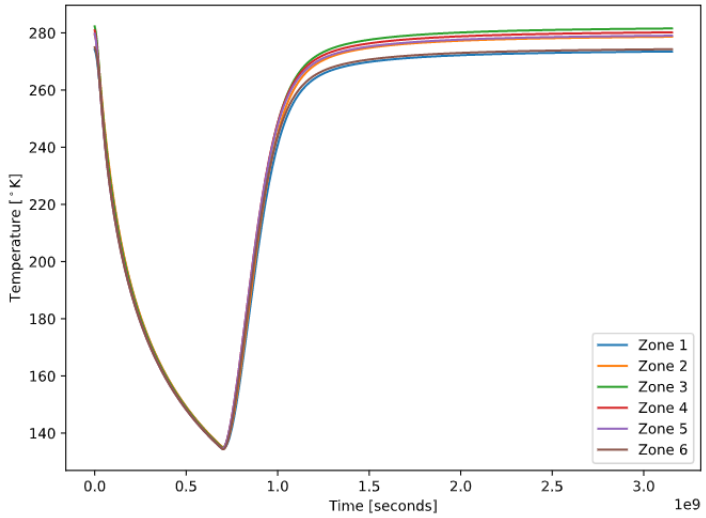

Figure 3: Reduction in solar forcing post eruption results in temperature drop.

2.3 Snowball Earth: Stochastic Volcanism and Temperature-Dependent Albedo

As a possible scenario for global glaciation, we couple a Poisson distribution of eruptions, both temporally and spatially, with a temperature-dependent parameterization of albedo. This coupling is shown in Figure 6, and will be discussed after looking at the mechanisms in isolation.

The interval post-origin for stochastic eruptive behaviour has been extended to 100 years visualize a return to equilibrium more clearly. From Figure 4, we see that following each eruption is a decline in zonal temperatures, and sufficiently close eruptions, in time, compound that effect. The distribution lag associated with aerosol spreading is still represented numerically, though a lag of a few months is difficult to discern visually on this extended time scale.

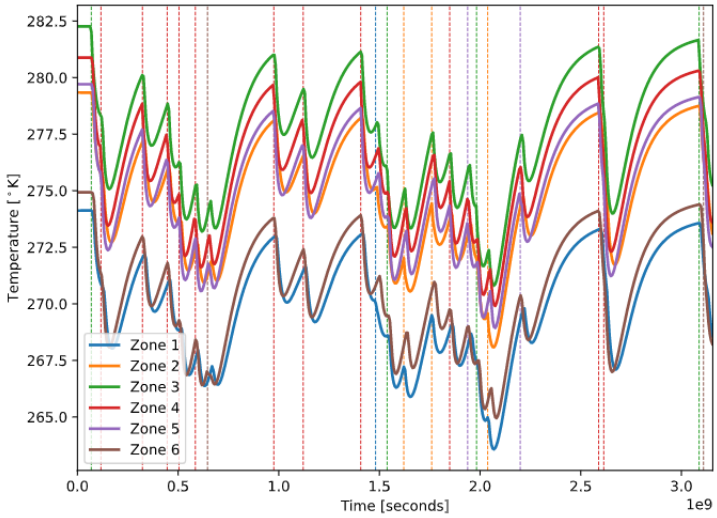

Figure 4: Stochastic eruption distribution following Poisson distribution. Vertical dotted lines are colored based on the zone the eruption occurred in, and their placement is the point in time at which the eruption is initiated.

To incorporate variable albedo, we define a piece-wise albedo parameterization dependent on zonal tem-

perature (Adapted from Jellinek 2020). The parameterization follows the form of Equation3 (Section 5.3.1), and ascribes behavior based on each zone's basal albedo and temperature range (Figure 5). Temperatures above $280°K$ allow each zone to take on their originally defined albedo, α_k (See Table 6). Temperatures below $250°K$ replace these with a constant ice albedo, while the interval between describes a quadratic growth from α_k to α_i as temperature declines.

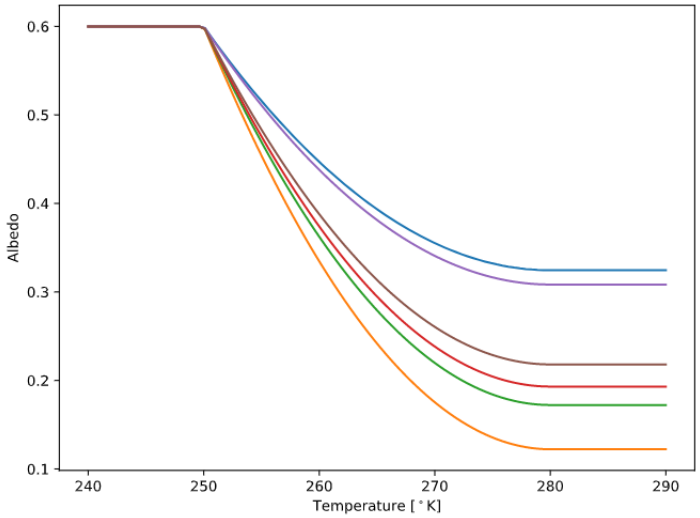

Figure 5: Albedo parameterization as a function of temperature in each zone.

By coupling these processes, and ranging through a series of initial temperature conditions in each zone, we are able to find a numerical snowball Earth in Figure 6. Similarly to our observations of Figure 4, eruptions that happen close in time have a compounded effect of driving temperatures down further. After several eruptions between $1.75e9 - 2.1e9$ seconds, this effect causes temperatures to drop below the lower threshold of our albedo parameterization, T_i and plummet to a new state between approximately $225 - 245°K$. This phenomenon will be expanded on in Section 3.3.

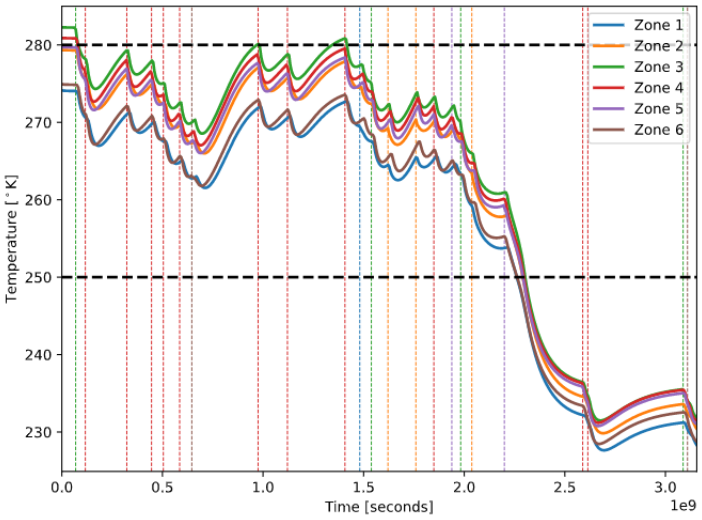

Figure 6: Integrating through climate model incorporating both stochastic volcanic eruptions and ice-albedo feedback parameterization.

3 Discussion

Here we will discuss the possible processes behind the numerical behavior of our Figures in Section 2 in order to elucidate the connection between our mathematical and computational results with their underlying physics.

3.1 Steady-State Climate Model: No Volcanism

Zones 4 and 5 experience a large initial temperature gradient due to a heat transfer coefficient indicative of Gulf Stream circulation processes that is larger than the transfer coefficients between other zones (Figure 1). This causes zones 4 and 5 to approach their equilibrium values more quickly. For example, zone 5 reaches its approximate equilibrium temperature within the first two months of the model year because the efficiency of heat transfer between these zones is greater than between others.

Zones 3 and 4 are the warmest zones due to their proximity to Earth's equator. Both lie within 30°N/S of the equator, and hence have the largest effective surface area, coupled with a low albedo due to a high land and sea fraction versus ice fraction (See Table 6). This increases these zones' retention of incoming solar radiative heating by reducing the amount lost to space as out-going, long-wave radiation (OLR). Zone 3 may be hotter than zone 4 due to smaller transfer coefficients between its adjacent zones than compared with zone 4, where heat transfer occurs rapidly due to influence from the Gulf Stream across the boundary of zone 4 and 5.

Conversely, zones 1 and 6 are the coldest zones at equilibrium due to their placement at Earth's high latitudes (> 60°N/S). This reduces their effective surface area such that less total solar insolation occurs, alongside a higher albedo due to a dominating ice fraction. This causes the OLR to be larger relative to incoming radiative heating than in the case of the other zones. Hence, temperature at equilibrium in zones 1 and 6 is lower. Zone 1 may be colder than zone 6 due to a higher albedo associated with a marginally larger ice fraction that increases OLR even relative to zone 6.

Comparing the solid and dashed lines in Figure 1, there is a general trend of reduced rate of change in temperature for several northern latitudinal zones. Zones 4 and 5 experience the greatest deviation from the original approach to equilibrium as this change is at their boundary of separation and directly reduces the amount of heat exchange between them. Zone 6 also experiences a reduction in the rate of approach to equilibrium due to its nonlinear relation with zone 5. As we can see, these effects are compounded in zones closest to zones 4 and 5, such that at sufficient separation, approaches to equilibrium are not noticeably affected. This is evident in zones 2 and 1, and suggests they have little dependence on temperature characteristics within the northern zones.

3.2 Climate Model Following Single Volcanic Eruption

3.3 Snowball Earth: Stochastic Volcanism and Temperature-Dependent Albedo

4 Conclusion

4.1 Future Work

5 Ancillary Information

5.1 Author Contributions

Section	Subsection	Contributors
Graphic	Box-Model	M
Code	Steady-State Climate	P and E
Code	Perturbation: Single Volcanic Eruption	P, E, and M
Code	Snowball Earth	P, E, and M
Introduction		M
Results	Steady-State Climate	n/a
Results	Perturbation: Single Volcanic Eruption	n/a
Results	Snowball Earth	n/a
Discussion	Steady-State Climate Model	n/a
Discussion	Perturbation: Single Volcanic Eruption	n/a
Discussion	Snowball Earth	n/a
Conclusion	Future Work	n/a
Conclusion	Summary	n/a

Table 1: In descending order: names depict relative contribution to sections with more than one contributor.

5.2 Algorithm Development

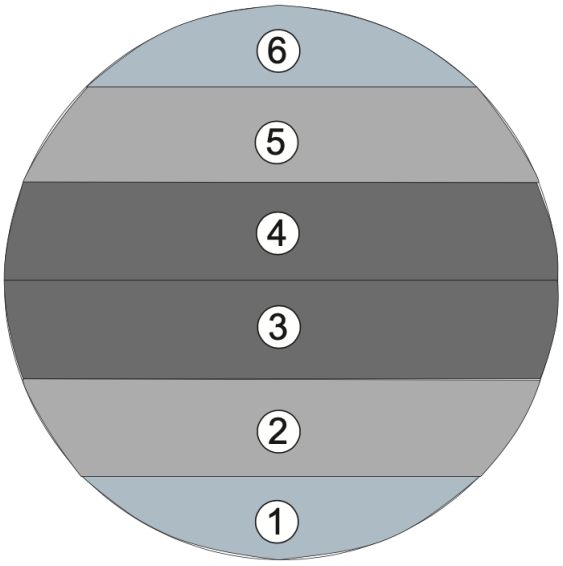

Figure 7: Graphic depicting zone intervals.

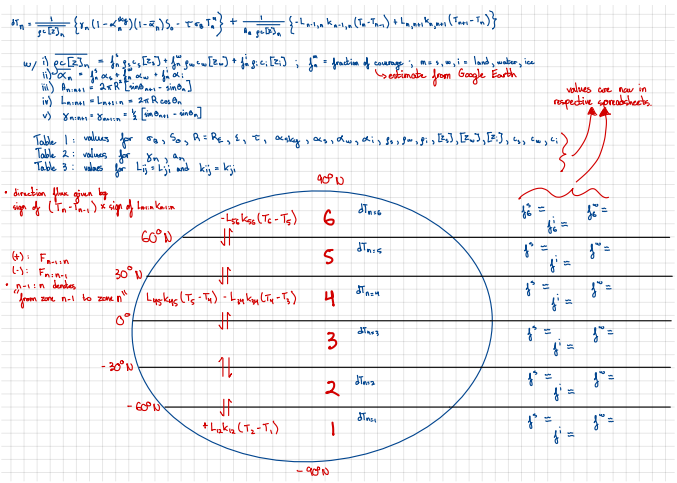

Figure 8: Sketch depicting zone intervals and necessary parameters for numerical solving.

1. Identify 6 latitudinal zones. Namely between $0-30°NS$, $30-60°NS$ and $60-90°NS$.
2. Determine parameters associated with each area.
3. Solve ODE numerically using Paul Matlashewski's ClimateModel.py library.

5.3 Data

5.3.1 Model Equations

$$\frac{dT_k}{dt} = \frac{1}{\rho_k c_k [Z_k]}\{\gamma_k(1-\alpha_k^{sky})(1-\bar{\alpha_k})S_0 - \tau\sigma_B T_k^4\} + \frac{L_{ki}k_{ki}}{A_k\rho_k c_k[Z_k]}(T_k - T_i) \quad k = 1,\ldots,6 \tag{1}$$

$$\frac{dT_k}{dt} = \frac{1}{\rho_k c_k [Z_k]}\{\gamma_k(1-\alpha_k^{sky})(1-\bar{\alpha_k})\phi_k(t)S_0 - \tau\sigma_B T_k^4\} + \frac{L_{ki}k_{ki}}{A_k\rho_k c_k[Z_k]}(T_k - T_i) \quad i \neq k, i = k \pm 1 \tag{2}$$

$$\alpha_k(T_k) = \begin{cases} \alpha_k & T_k \geq T_0 \\ \alpha_k + (\alpha_i - \alpha_k)\frac{(T_k - T_0)^2}{(T_i - T_0)^2} & T_i < T_k < T_0 \quad T_i = 250°K \quad T_0 = 280°K \\ \alpha_i & T_k \leq T_i \end{cases} \tag{3}$$

5.3.2 Equilibrium Temperatures: Steady State Model

Table 2: Inter-zonal heat transfer suppressed

Zone	Equilibrium Temperature [°K]
1	217.23
2	279.74
3	296.45
4	294.56
5	263.56
6	225.33

Table 3: Inter-zonal heat transfer allowed

Zone	Equilibrium Temperature [°K]
1	274.12
2	279.34
3	282.26
4	280.88
5	279.71
6	274.93

5.3.3 Eruption Times Series

Table 4: Eruption Times Series 1

date	value
1982.396551724138	347.0380363253488
1982.4827586206898	369.1787312450645
1982.5689655172414	384.4491971571466
1982.683908045977	407.35434763534266
1982.8275862068965	439.42090023690446
1983	479.12213740458014
1983.603448275862	488.3054751250329
1983.9195402298851	499.7679213828201
1984.6379310344828	506.6655698868123
1985.6149425287356	518.9166008598754
1986.3620689655172	521.2351934719663
1987.1666666666667	526.6094147582697
1988	526.6412213740458
1988.7183908045977	527.4319996490304
1990.3850574712644	525.9688953233307
1991.0747126436781	529.8120119329649

Table 5: Eruption Time Series 2

date	value
1991.6781609195402	390.1403878213565
1991.8793103448277	412.28546986048957
1992.1954022988507	439.7784504694218
1992.4540229885058	464.21580240414147
1993.1436781609195	502.4100640519435
1993.8333333333335	516.940203562341
1994.6954022988507	523.843335965605
1995.7298850574714	527.6996139334913
1996.9655172413793	530.800210581732
1998.057471264368	532.3686057734492
1998.4597701149426	531.6206019127841

5.3.4 Parameters

Table 6: Zonal Parameters

	Parameter	Value
Zone 1	Geometric Factor	0.1076
	Area Fraction	0.067
	Land Fraction	0.0
	Ocean Fraction	0.550925926
	Ice Fraction	0.449074074
Zone 2	Geometric Factor	0.2277
	Area Fraction	0.183
	Land Fraction	0.074074074
	Ocean Fraction	0.925925926
	Ice Fraction	0.0
Zone 3	Geometric Factor	0.3045
	Area Fraction	0.25
	Land Fraction	0.240740741
	Ocean Fraction	0.759259259
	Ice Fraction	0.0
Zone 4	Geometric Factor	0.3045
	Area Fraction	0.25
	Land Fraction	0.3101851851
	Ocean Fraction	0.689814815
	Ice Fraction	0.0
Zone 5	Geometric Factor	0.2277
	Area Fraction	0.183
	Land Fraction	0.694444444
	Ocean Fraction	0.305555556
	Ice Fraction	0.0
Zone 6	Geometric Factor	0.1076
	Area Fraction	0.067
	Land Fraction	0.277777778
	Ocean Fraction	0.652777778
	Ice Fraction	0.069444444

Table 7: Global Parameters

Parameter	Value	Units
Stefan-Boltzmann Constant	5.6696e-8	$Wm^{-2}K^{-4}$
Solar Constant	1368	Wm^{-2}
Earth Radius	6371e3	m
Earth Total Emissivity	1	
Atmospheric Transmissivity	0.63	
Atmospheric Albedo	0.2	
Land Albedo	0.4	
Ocean Albedo	0.1	
Ice Albedo	0.6	
Land Density	2500	kgm^{-3}
Ocean Density	1028	kgm^{-3}
Ice Density	900	kgm^{-3}
Land Thermal Scale Depth	1.0	m
Ocean Thermal Scale Depth	70.0	m
Ice Thermal Scale Depth	1.0	m
Land Specific Heat Capacity	790	$JkgK^{-1}$
Ocean Specific Heat Capacity	4187	$JkgK^{-1}$
Ice Specific Heat Capacity	2060	$JkgK^{-1}$

6 References

References

Budyko, M. (Dec. 1969). "The effect of solar radiation variations on the climate of Earth". In: *Tellus* 21, 5, pp. 611–619. URL: https://doi.org/10.3402/tellusa.v21i5.10109.

Jellinek, M. (Nov. 2020). "Volcanic Eruptions and Climate Change". In: *EOSC 453* At: University of British Columbia, Vancouver, Canada.

Robock, A. (May 2000). "Volcanic eruptions and climate". In: *Reviews of Geophysics* 38, 2, pp. 191–219.